



Changes in the fractal and electronic structures of activated carbons produced by ultrasonic radiation and the effect on their performance in supercapacitors

B.Ya. Venhryn^{a,*}, I.I. Grygorchak^a, Z.A. Stotsko^a, Yu.O. Kulyk^b, S.I. Mudry^b, V.V. Strelchuk^c, S.I. Budzulyak^c, G.I. Dovbeshko^d, O.M. Fesenko^d

^a Lviv Polytechnic National University, 12 St. Bandera Street, Lviv 79013, Ukraine

^b Ivan Franko National University of Lviv, 8 Kyrylo and Mefodiy Street, Lviv 79005, Ukraine

^c V. Lashkaryov Institute of Semiconductor Physics, National Academy of Science of Ukraine, 41, pr. Nauky, Kyiv, 03028, Ukraine

^d Institute of Physics, National Academy of Science of Ukraine, 46, pr. Nauky, Kyiv 03028, Ukraine

* Corresponding e-mail address: venhryn_b@ukr.net

Received 09.07.2012; published in revised form 01.09.2012

ABSTRACT

Purpose: Effect of ultrasonic irradiation on change of electron structure as well as fractal one of activated carbons and motivation that these changes are most responsible for the improvement of functional parameters in supercapacitors, were the aim of this paper.

Design/methodology/approach: Experimental studies were carried out by means of impedance spectroscopy, cyclic voltammetry, X-Ray diffraction, small angle X-Ray diffraction, X-Ray photoelectron spectroscopy, IR-spectroscopy, Micro-Raman spectroscopy and galvanostatic cycling methods.

Findings: Ultrasonic modification of carbon is effective method to increase the specific capacitance as well as power of carbon-based supercapacitors. Changes of parameters of double electric layer are tightly related with change of fractal dimension and allow increasing the percolate mobility of charge carries.

Research limitations/implications: This research is a complete and accomplished work.

Practical implications: Carbon materials, modified by ultrasonic irradiation, can be used as promising electrode materials in energy storage devices of new generation.

Originality/value: This work is of urgent importance for studying of physical and chemical processes in energy storage systems. It is shown that method of ultrasonic irradiation is highly effective for modification of carbon-based materials as electrodes in supercapacitors.

Keywords: Ultrasonic radiation; X-ray small angle scattering; Nanocluster; Nanoporous carbon; Supercapacitor

Reference to this paper should be given in the following way:

B.Ya. Venhryn, I.I. Grygorchak, Z.A. Stotsko, Yu.O. Kulyk, S.I. Mudry, V.V. Strelchuk, S.I. Budzulyak, G.I. Dovbeshko, O.M. Fesenko, Changes in the fractal and electronic structures of activated carbons produced by ultrasonic radiation and the effect on their performance in supercapacitors, Archives of Materials Science and Engineering 57/1 (2012) 28-37.

PROPERTIES

1. Introduction

Nowadays, the development of electric vehicles production and alternative energetics makes demands on creation of highly powerful systems of accumulation and storage of energy. Significant efforts in this direction though and allowed to increase the voltage to 4.5-4.7 V, but their specific capacitance remains low.

On that reason it is of high importance to improve the properties of functional materials, which determine the working parameters of mentioned above systems. Such problem is general for various materials, especially with nanoscale structure and is extensively studied in present time, for instance in [1, 2].

Overcoming this problem can be achieved using supercapacitors with caactive or pseudocapacitive energy storage mechanism. However, the key to success in this endeavor is to ensure the combination of optimal porous structure with corresponding electronic structure of the material that provides unblocking of Helmholtz capacitance by capacitance of spatial charge region in solids. Commonly used for this purpose methods of chemical modification of the porous structure [3-5] do not give the desired simultaneous changes of the electronic structure. For this reason, in this paper, we try to solve the mentioned above problem, since a significant number of works on improvement of active materials of supercapacitors unreasonably associated only with the modification of their porous structure [6-9] or connecting to the surface of certain functional redox groups [10-12] without adequate attention to providing the necessary electronic structure. We hope that more effectiveness of energy storage systems can be reached by means of ultrasonic treatment that is the motivation of investigation on influence of ultrasonic irradiation on supercapacitor parameters.

2. Backgrounds and experimental

It is clear that electric double layer (EDL) is the main functional element in physical-chemical processes, occurring in supercapacitors. Obviously that concept approach on this problem is supposed to be related with structure features of EDL, created at the electrolyte-nonmetallic solid phase interface (Fig. 1a). This interface supposes the presence in this circuit (Fig. 1b) the capacitance of volume charge region (VCR) of solid phase – C_{SC} region, which can block the Helmholtz capacitance.

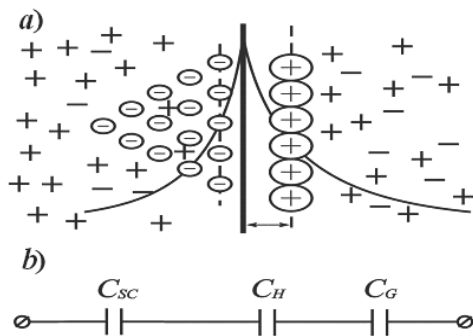


Fig. 1. Electric double layer model for nonmetallic electrodes – a) and equivalent electric circuit – b)

According to circuit, which is shown in Fig. 1b, the total capacitance of EDL equals:

$$C^{-1} = C_{SC}^{-1} + C_H^{-1} + C_G^{-1}, \quad (1)$$

where C_H – Helmholtz capacitance. Commonly the Gouy-Chapman capacitance of diffusive layer in electrolyte C_G , significantly prevails the capacitance of dense part of EDL, which is known as Helmholtz layer. Noted problem of blocking in fact is absent for metallic electrodes, whereas it is actual for carbon-graphite ones due to significant value of Debye screening radius. It is clear that unblocking of Helmholtz capacitance promotes the increase of C_{SC} , which is proportional to density of states for delocalized charge transfers at Fermi-level $N(E_F)$ in accordance to well known relation [13]:

$$C_{SC} = e_0 \{ \epsilon_{SC} \epsilon_0 N(E_F) \}^{\frac{1}{2}}, \quad (2)$$

where ϵ_{SC} – relative permittivity of volume charge region, ϵ_0 – permittivity for vacuum, e_0 – charge of electron.

Just increase of C_{SC} should be the result of modification, but not alone. On other hand, the higher concentration of charge carries causes the higher degree of charge screening that is the main reason of more density in EDL, increasing in such way the capacitance of Helmholtz layer.

For this purpose we propose a new mechanism of ultrasonic modification, main idea of which is in changing of fractal structure with mediate effect on electron structure that occurs due to cumulative action [14] on the nanoporous structure of carbon, as well as cavitation processes and direct ultrasonic influence on subsystem of impurities [15].

We have used the carbon with nanoporous structure ($S_{act} = 467 \text{ m}^2/\text{g}$, maximum of pore diameter distribution function $d = 1.5 \text{ nm}$). The ultrasonic irradiation was carried out by means of ultrasonic disperser in aqueous medium at frequency 22 kHz. Both aqueous (30% KOH) and nonaqueous (1 M $(\text{C}_2\text{H}_5)_4\text{NBF}_4$ in acetonitrile) solutions were used as electrolyte systems for molecular energy storage devices.

In order to study the porous structure of materials under investigation we have used the method of X-Ray small angle scattering. Investigation was carried out with using DRON 3 powder diffractometer ($\text{Cu-K}\alpha$ radiation, $\lambda = 1.5418 \text{ \AA}$). The single crystal of Ge was used to obtain the monochromatized radiation by reflecting from (111) - planes. In order to restrict the parasitic scattering from crystal-monochromator and reduce scattering phone the special slit units were installed before the sample and detector which have $\pm 4 \text{ mm}$ shift in perpendicular to initial beam direction. Using of Ge perfect single crystal and focusing system for initial and diffracted beam allowed us to measure the small-angle X-Ray spectra starting from wave-vector $s = 0.01 \text{ \AA}^{-1}$. The slit of 0.1 mm width, that corresponds the volume resolution $\Delta(2\theta) = 0.03^\circ$ was installed before detector. Scattered intensity was recorded in scanning regime within angle interval $0.25 - 4.00^\circ$ with step 0.05° and exposition 100 s. In case of investigation in wide angle range the slit of 1.00 mm width was installed before detector. Peak positions in diffraction patterns have been determined with accuracy $\approx 1-2\%$ whereas other structure parameters such as size of nanoparticles, fractal dimension value and their

fraction in material have been estimated from intensity curves with accuracy 3-5 %.

Electrochemical investigation of activated carbon was carried out by means of three-electrode cell with chlorine-silver reference electrode. Impedance measurements were done within (10^{-2} - 10^5 Hz) frequency region with using "AUTOLAB" ("ECO CHEMIE" Holland) of measuring system, attached with FRA-2 and GPES software. Creation of impedance models was realized using the ZView 2.3 (Scribner Associates) software. Cyclic voltamperograms of electrochemical cells were recorded with scan rate 0.01 V/s. Charge-discharge galvanostatic cycles were maintained by means of electronic galvanostatic unit.

Electron structure of nanoporous carbon before and after ultrasonic modification has been investigated by means of X-ray photoelectron spectroscopy with using Kratos Axis Ultra X-ray photoelectron spectrometer and combination scattering spectroscopy by means of triple spectrometer Jobin-Yvon/Horiba T64000. The possible influence of surface functional groups was checked by means of IR-spectroscopy with using of IR-Fourier spectrometer Bruker IFS 66.

Micro-Raman measurements were carried out in the backscattering geometry at room temperature using above mentioned spectrometer and thermoelectrical-cooled charge-coupled device (CCD) detector. Ar+/Kr+ laser (488.0 nm) was used as excitation source. The laser power was changed in the range of 0.25 - 25 mW. The samples were placed on a computer-controlled XY table with a displacement step of 0.1 μm . The Olympus BX41 confocal optical microscope equipped with a $\times 100$ (numerical aperture $NA = 0.90$) was used to focalize the laser light on the sample and collect the scattered light to the spectrometer. A 100 μm confocal diameter diaphragm was placed at the back focal plane of the objective provided the lateral submicron resolution of the measurements.

3. Results and discussion

The influence of ultrasonic waves on supercapacitor parameters should be analyzed starting from diffraction data. Diffractions patterns for carbon before and upon ultrasonic treatment during 5, 10, 15 and 20 min show the similar features, which are not observed for initial material. The intensity curves, corresponding to such diffraction patterns and obtained when treatment was done in volume of dispersive medium 50 ml are shown in Fig. 2.

Wide diffraction maxima with untypical for crystalline materials profile, indicate the existence of amorphous structure for both initial and treated samples. This maximum corresponds to interlayer distance in graphite structure. It is seen that principal peak position shifts to large wave vector values when duration of treatment is 5 and 10 min. With next treatment duration increase to 15 and 20 min this parameter shifts in opposite direction and attains the value, which is somewhat less than for initial material. Such behavior means that in real space the interlayer distance decreases at short treatment duration and then increases at more long duration.

By means of Debye-Scherrer formula the mean radius of initial carbon nanoparticles has been determined from the half width of principal peak:

$$r_0 = \frac{\lambda}{2\beta \cos(\theta)}, \quad (3)$$

where β – half width of diffraction maximum, θ – half of scattering angle.

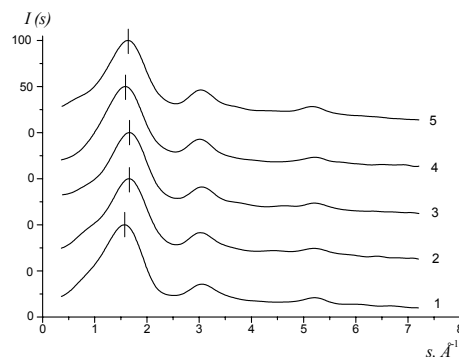


Fig. 2. Diffraction patterns for initial carbon – (1) and after ultrasonic treatment during 5 – (2), 10 – (3), 15 – (4) and 20 min – (5) in volume of dispersive medium 50 ml

Small angle scattering curves for carbon upon ultrasonic treatment during 5 min at different volumes of H_2O are shown in Fig. 3a. As is seen the linear dependence of scattered intensity is observed over wide range of wave vector [s_0, s_{max}] ($s_{max} = 0.327 \text{ \AA}^{-1}$). Thus $I(s)$ dependence is a function $I(s) \sim s^{-n}$, where n varies within interval $2 < n < 3$, that indicates the fractal structure of graphite. We can state that within above mentioned range of wave vector X-ray small angle scattering is formed from carbon nanoclusters, which are volume fractals, created from initial carbon nanoparticles. Low limit of wave vector interval s_0 allows determining the mean radius of fractal cluster:

$$R_f = \frac{\pi}{s_0} \quad (4)$$

At the same time it is known [16] that fractal cluster density depends on its size as:

$$\rho_f = \rho_0 \left(\frac{R_f}{r_0} \right)^{(D_f - 3)} \quad (5)$$

where $D_f = n$ - fractal dimension, ρ_0, r_0 - density and radius of initial materials, respectively. Using the equations (4) and (5) we obtain the formula for specific surface area:

$$S = \frac{3}{\rho_f R_f} = \frac{3}{\rho_0 R_f} \left(\frac{R_f}{r_0} \right)^{(3 - D_f)} \quad (6)$$

Parameters of fractal structure, calculated by means of formula (3) - (6) for carbon upon ultrasonic treatment are listed in Table 1.

Increasing of H_2O volume during ultrasonic treatment leads to sensible changes in small angle scattering spectra. Particularly s_0 shifts to larger values, that is related with decrease of fractal cluster radius (Table 1). Some changes are observed also for fractal dimension, namely its increase to $n = 2.74$ for H_2O volume 200 ml at 5 min irradiation duration.

Table 1. Parameters of fractal structure for carbon after ultrasonic treatment

Ultrasonic treatment duration, min	$V(\text{H}_2\text{O})$, ml	r_o , Å	R_f , Å	D_f	S_2 , m ² /g
5	50	9.0	98	2.55	367
	100	10.5	87	2.52	445
	200	10.0	80	2.74	332
10	50	8.5	115	2.59	378
	100	11.0	97	2.46	580
	200	10.0	142	2.56	363
15	50	11.0	28	2.36	579
	100	9.5	25	2.23	589
	200	11.0	22	2.16	654
20	50	10.0	25	2.77	600
	100	10.0	40	2.49	780
	200	10.0	35	2.53	665

Increase of treatment duration to 10 min does not cause the significant changes in scattered curves (Fig. 3b). Values of fractal dimensions vary within range 2.46 - 2.59 whereas the radius of fractal clusters increases from 97 Å to 142 Å. It should be noted

also that feature of previous increase of D_f with increasing of H_2O volume (Table 1) is another.

More significant changes of fractal structure are observed in samples under investigation upon ultrasonic treatment during 15 min (Fig. 3c) and 20 min (Fig. 3d). Scattering curves, represented in double logarithmic coordinates, reveal two regions with different slope. This slope within $[s_o, s_{max}]$ range for 15 min regime is equal to dimension of Euclidian space ($n=3$). It can be supposed that within this angular interval the scattering curve is formed by carbon nanoclusters, which do not reveal the fractal structure and are rather related with dense packed agglomerate of initial carbon nanoclusters. The slope of this curve within $[s_{min}, s_o]$ range decreases and lies in interval $2 < n < 3$ that, as was mentioned above, is typical for scattering from fractal aggregates of volume kind, whose elements are carbon clusters of R_f radius. It should be noted also, that in this case the increase of H_2O volume promotes the decrease both of fractal dimension (from 2.36 to 2.16) and size of carbon clusters (from 28 Å to 22 Å).

Special attention is paid to analysis of small angle scattering spectra of materials upon ultrasonic treatment during 20 min. In this case for $[s_o, s_{max}]$ range the index n is about 4 indicating the scattering from homogeneous spherical particles with smooth surface, which is commonly interpreted by Porod law [17].

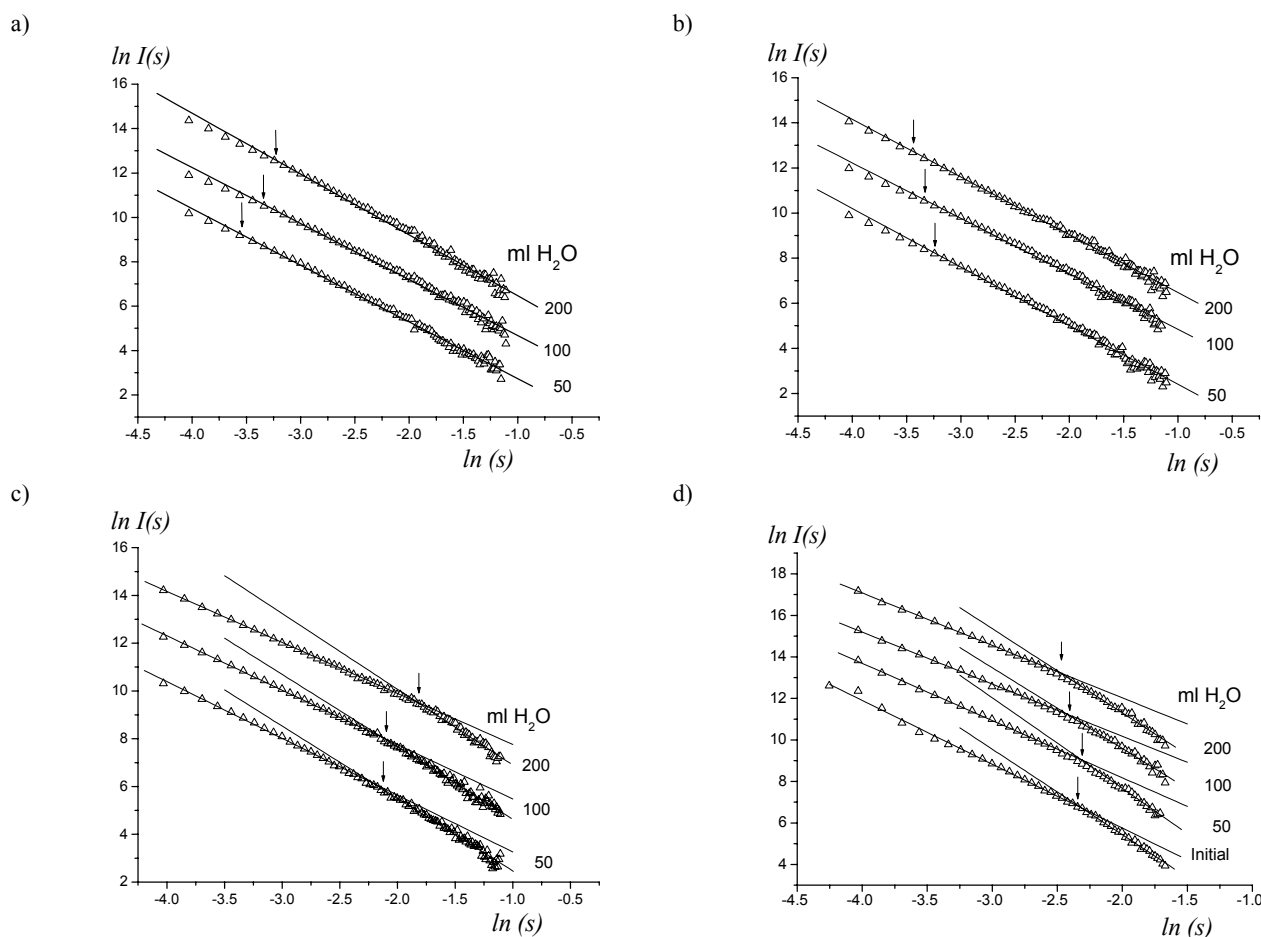


Fig. 3. Dependence of X-ray scattered intensity versus wave vector after ultrasonic treatment during 5 – a), 10 – b), 15 – c) and 20 min – d)

At space scales $R > R_s$ (where R_s is radius of surface fractal clusters) the nanoparticles form the volume fractal aggregates. The increase of H_2O volume to 100 and then to 200 ml leads the growth of n to 3.45 and 3.70, respectively. Since in this case $3 < n < 4$ one can assert the presence of nanoparticles with unsmooth surface and fractal dimension $D_s = 6 - n$. In this case the surface area of fractal aggregates of this kind equals [16]:

$$S = 4\pi r_0^2 \left(\frac{R_s}{r_0} \right)^{D_s} \quad (7)$$

Since that fractal dimension $D_s > 2$ follows that these fractals have larger value of surface area in comparison to particles with smooth surface ($D_s = 2$). On other hand, the specific surface area for fractal aggregates, created from clusters with unsmooth surface equals:

$$S = \frac{3}{\rho_0 R_s^3} r_0^2 \left(\frac{R_s}{r_0} \right)^{D_s} \quad (8)$$

Calculated results are listed in Table 1. Change of small angle scattering parameters is accordance with results illustrated in Fig. 2.

Therefore, one can assert that dominant factor of specific surface influence is an ultrasonic treatment duration, which, first of all, is related with the change of fractal structure of carbon nanoclusters. On that reason we shall put aside the influence of dispersion surrounding volume, suggesting that this problem will be the subject of further studies. Instead of this problem, the main attention we focus on understanding of influence of ultrasonic treatment duration, for instance at volume of 50 ml of H_2O , since feature of $S(t)$ change is correlated for investigated volumes (Table 1).

Comparing the obtained characteristics for fractal structure with data on galvanostatic “charge-discharge” cycles (Fig. 4), one can see the inconsistency between S and C , whose non monotone behavior most probably indicate the blockade of Helmholtz layer capacitance by of VCR capacitance.

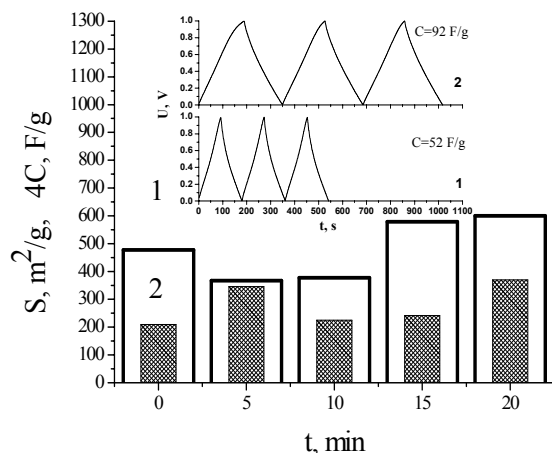


Fig. 4. Specific surface (1) and specific capacitance of galvanostatic discharge (2) as a function of ultrasonic irradiation duration

In inset to this figure the “charge-discharge” curves reveal the increase of specific capacitance from 52 F/g to 92 F/g after ultrasonic modification during 20 min in 50 ml of H_2O . The motive for such assertion are the infrared spectra (Fig. 5), which exclude the contribution to increase of specific capacitance after ultrasonic modification related with pseudocapacitance from surface functional groups, since the intensity of all absorption band decreases without appearance of new ones. Thus, new states of H-bonded C=O (1746, 1711 cm^{-1}) with less intensity have appeared in the sample after ultrasonic treatment. In initial sample the position of C=O has position at 1742 cm^{-1} . In the region of 1600-1700 cm^{-1} we observed 2 peaks at 1632 cm^{-1} (C=C and H_2O vibration) and 1660 cm^{-1} (C=C) in initial sample. After ultrasonic treatment the band at 1660 cm^{-1} disappeared and other band splitted into 2 bands- 1640 cm^{-1} (C=C) and 1626 cm^{-1} (H_2O) with less intensity. We suppose that a number of defects in rings, decreases in the sample after ultrasonic treatment (e.g. for C=C bonds in open ring). In the same time we have observed a wide band in the range of 1300-750 cm^{-1} , where the number of different states of C-C bond became more after treatment. This fact could be explained by appearance a great number of short fragments of graphite net with less defects and correlate with Raman data presented lower. We have registered a decrease of CH_2 and CH_3 in the region of stretching vibration and increase of ratio of CH_2/CH_3 in the sample after treatment, that is an evidence of decrease of CH_3 broken bonds in the graphite domens. After ultrasonic treatment a number of broken states and sp^3 states became less.

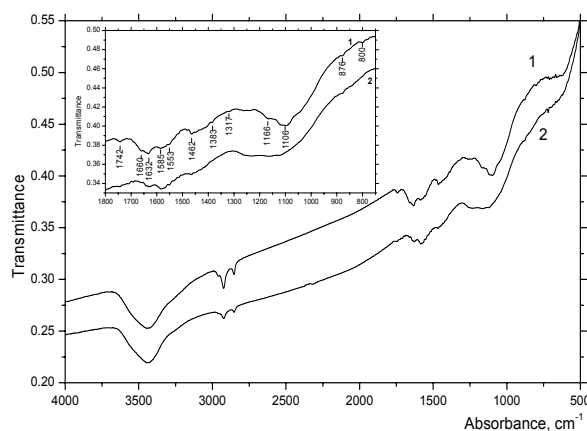


Fig. 5. Infrared spectra of carbon: 1 – initial sample; 2 – after 20 min of ultrasonic modification in dispersive medium volume 50 ml

Data of impedance spectroscopy also are the one more motivation of this. First of all it should be noted that Nyquist plots for all parameters of modification have typical shape (Fig. 6), which shows some distributed capacitance.

That, as well as necessary to account the capacitance of VCR, need to use de Levie model [18], modified by series connection of parallel $R_{SC}C_{SC}$ -chain, as it is shown in inset to Fig. 6, at construction of adequate impedance model. Here R_{SC} and C_{SC} -resistance and capacitance of VCR respectively. Results of computer parametric identification are shown as histograms (Fig. 7), where C_H means the capacitance of Helmholtz layer.

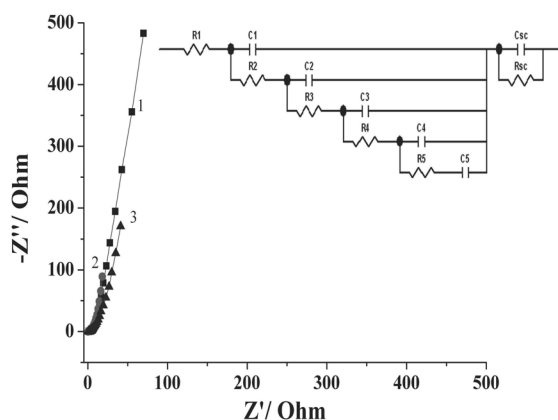


Fig. 6. Nyquist plots of carbon: 1 – initial sample; 2 – after 5 min of ultrasonic irradiation in 50 ml H₂O; 3 – after 20 min of ultrasonic irradiation in 50 ml (inset to figure – the equivalent electric circuit)

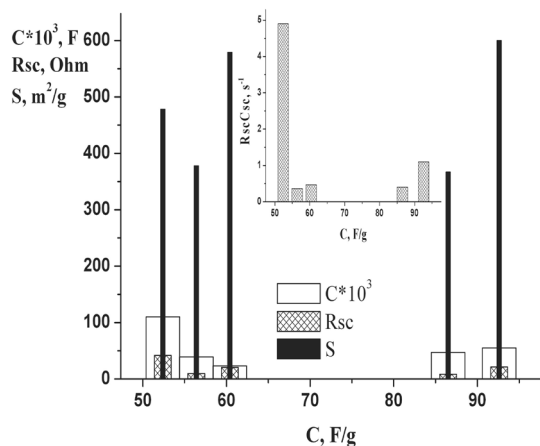


Fig. 7. Parameters correlation for double electric layer and values of specific capacitance for galvanostatic discharge

It should be noted that ultrasonic irradiation leads to reduction of C_{SC} (non-monotone with increasing both t and C), indicating according to (2) the decrease of density of states on Fermi level. Direct experimental confirmation of this was obtained in our studies by means of X-ray emission spectroscopy. Spectrum of valence band for initial activated carbon (Fig. 8a) shows the two shoulder profile with significant reduction of intensity at reaching of bonding energy to Fermi level. This intensity on Fermi level is proportional to electron density and equals $I(E_F)=13630$. After ultrasonic treatment the shape of valence band is not changed (Fig. 8b), but sensible reduction of intensity on Fermi level to $I(E_F)=9300$ occurs.

At the same time it can be seen that ultrasonic treatment also caused the reduction of R_{SC} with non-monotone behavior, which is unidentical to one for C_{SC} , that does not correlate with decreasing of $N(E_F)$. Therefore, the reduction of C_{SC} and R_{SC} shows no relations with decreasing of measured specific discharge capacitance C in galvanostatic “charge-discharge” cycles (Fig. 7).

This gives the motive to assert that most responsible for C is the factor of time constant $R_{SC}C_{SC}$ – chain (insert to Fig. 7), which in fact means the following:

- shunting of C_{SC} by resistance of VCR region, so in this case R_{SC} notes the fact, that effective unblocking of Helmholtz capacitance occurs, when the plate charging time is larger than period of its oscillations R_{SC} ;
- symmetrization of voltage-current characteristic for regions of cathode and anode polarization.

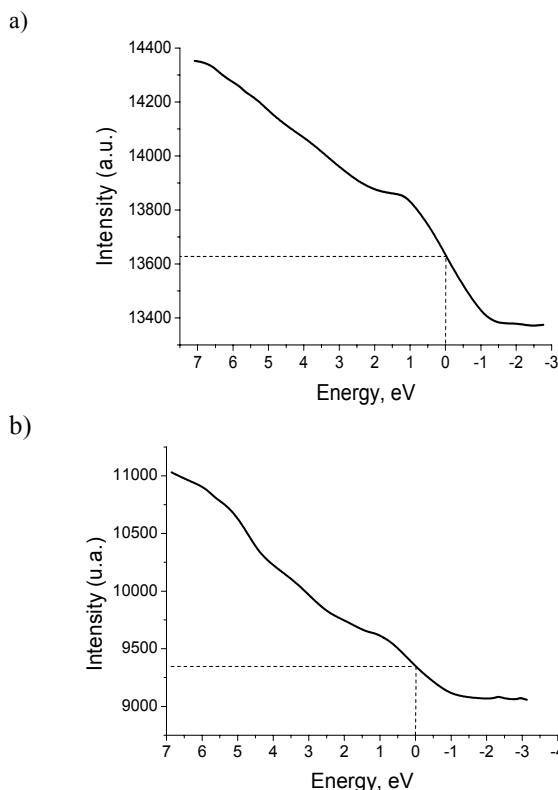


Fig. 8. Intensity of valence band for a) initial carbon and after ultrasonic treatment during 20 min in dispersive medium volume 50 ml b)

Therefore, values of measured capacitance correlate with parameters of EDL in untypical way. Data, obtained for materials under investigation allow supposing that in hierarchic aspect for the same values of active surface areas the most effective unblocking of Helmholtz capacitance is due to the low value of resistance for VCR (insert to Fig. 7).

Proposed mechanism is most acceptable for organic electrolyte solution (1 M (C₂H₅)₄NBF₄ in acetonitrile). Here is a slight increase of specific capacitance for all parameters used at ultrasonic irradiation. But maximum (20 %) value of C in comparison with initial sample can be reached for duration of $t=10$ min and $t=15$ min for volume of dispersion medium 50 ml and 100 ml, respectively. Just at these parameters the $R_{SC}C_{SC}$ – factor and reduction of Helmholtz capacitance are minimum. It should be noted here that in this case, contrary to aqueous solution of potassium hydroxide, C_H for all parameters of ultrasonic irradiation decreases, that at taking

into account the data on S increasing, indicates the shift of maximum in pores distribution function to smaller values that is confirmed by data of precision porometry.

Taking into account that genesis of porosity depends on kind of raw after activation carbonization; one can suppose that ultrasonic treatment is effective also for carbon materials of another origin. Really, for activated carbon, obtained from apricot stones after 5 min of irradiation in 100 ml of dispersion medium, about 30 % increase of discharge galvanostatic specific capacitance for 1 M $(C_2H_5)_4NBF_4$ in acetonitril occurs.

Concerning to physical nature of observed changes, we select at least two aspects:

- we deal with untypical for carbon materials phenomena stimulated by ultrasonic irradiation, which are typical for semiconductors [15]. Consequently, such ultrasonic treatment can be used for redistribution of impurities and in result for modification of impurity energetic topology;
- strong dependence of mobility and may be also hydrophilic nature from fractal structure.

Studies of microstructure also have been carried out by means of scanning microscopy. Data of both quantitative and qualitative analysis of carbon materials before and after ultrasonic treatment in different regimes by means of JEOL JSM-6490LV scanning microscope is the direct confirmation first of these two aspects. It was found that ultrasonic irradiation slightly changes the dispersivity and morphology of particles. At the same time this irradiation essentially decreases the number of impurities in near-surface layers of material (Fig. 9).

In Table 2 the distribution of chemical elements, which material consists is presented. In other words we can control the surface electron states, created by impurities as well as by native defects by means of ultrasonic irradiation.

Table 2.
Distribution of chemical elements before- and after ultrasonic treatment of carbon material

Element	weight % (± 0.1 %)		atomic % (± 0.1 %)	
	initial	after ultrasonic treatment	initial	after ultrasonic treatment
C	91.5	95.0	94.3	96.3
O	6.5	4.7	5.0	3.6
Mg	0.2	-	0.1	-
K	1.2	-	0.4	-
Ca	0.6	0.3	0.2	0.1
Total	100.00	100.00	100.00	100.00

Another aspect of physical nature of observed changes means that dominant contribution to R_{SC} is not contribution from delocalized electrons, but from mobility, which should be attributed to kind of fractal structure. This is good illustrated in Fig. 7, where values of C_H and S are compared.

We have studied the short range ordering structures of the charcoal *in situ* by means of confocal micro-Raman spectroscopy and the effect of different ultrasonic exposure. Figure 10 shows such corresponding Raman spectra of the carbon, measured with a laser excitation wavelength of 488 nm (2.54 eV).

It was found that the Raman spectra of the untreated carbon consist of three major groups of bands (Fig. 10, curve 1). The first group includes two main intense first-order Raman bands at about

1360 and 1580 cm^{-1} , which correspond to the D- and G-vibrational mode of partially graphitized materials, respectively [19, 20].

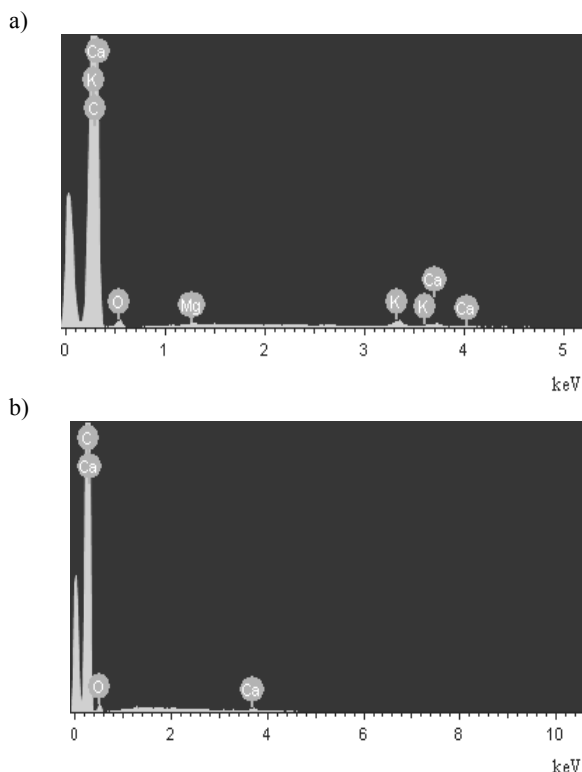


Fig. 9. Distribution of elements in initial carbon material a) and after ultrasonic treatment b)

Owing to the amorphous character of the carbon with a main sp^2 hybridization character, Gaussian fitting functions have been chosen for the analysis of Raman peaks. By fitting G and D bands, I_D/I_G ratio was obtained to be equal 2.2, indicating a substantial amount of distortion of bond lengths and angles [21]. In addition, the D_2 band, which corresponds also to the disordered induced phase, is observed at around 1620 cm^{-1} (Fig. 11). A weak peak at about 1210 cm^{-1} was observed as a shoulder D-band (see insert Fig. 10), the assignment of which is not straightforward. M. Armandi et al. [22] assigned a band at 1210 cm^{-1} to a C-O stretch of C-O-H surface groups.

The second frequency region (at 1900-2200 cm^{-1}) consists strongly asymmetric and wide band (we will refer to it as "C" peak [23]). This weak peak can be satisfactorily fitted by two Gaussian lines centered at around 2100 and 1980 cm^{-1} (Fig. 12a). These two components of the C peak in the Raman spectra confirm the formation of a carbon with a substantial presence of sp linear structures among a sp^2 hybridized disordered network [23]. It is also reasonable to assume the presence of a large quantity polyene and polycumulene moieties coexisting in the films, giving origin to the vibrational frequencies of the C-C bond in both type chains at 2100 and 1980 cm^{-1} , respectively. Because Raman cross section of linear chains in the carbon amorphous network is not known, an accurate quantitative determination of

the sp content with respect to sp^2 is not possible by Raman spectroscopy [24]. At the same time, we have observed the complete disappearance of the two components of the C peak after ultrasonic treatment (Fig. 12b).

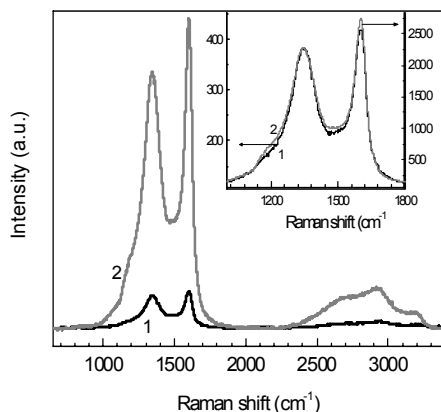


Fig. 10. Raman spectra of initial carbon (1) and after ultrasonic treatment in 50 ml H₂O during 5 min (2) at $\lambda_{exc}=488$ nm. Insert shows spectra of the D and G spectral regions (900-1800 cm⁻¹) which are normalized to intensity D-peak

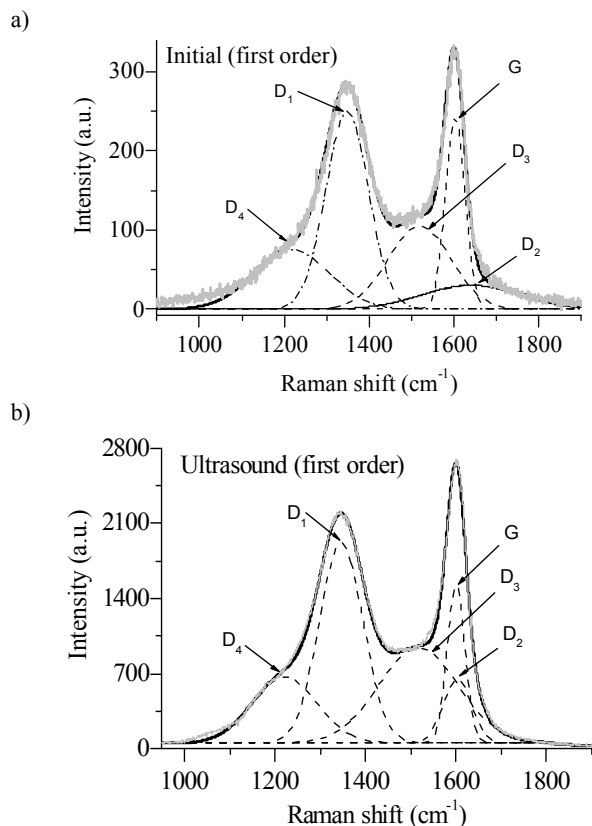


Fig. 11. First order micro-Raman spectra of carbon: a) before and b) after ultrasonic modification. G, D1, D2 bands fitted by Lorentz functions, D3, D4 - Gaussian functions

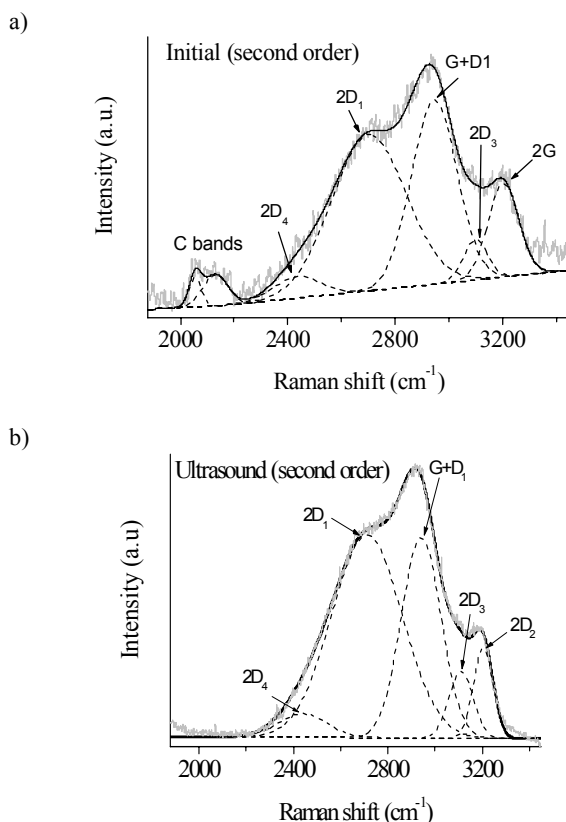


Fig. 12. Second order micro-Raman spectra of carbon: a) before and b) after ultrasonic modification

Thus, during this process ultrasonic treatment can induce the rearrangement and ordering of a local region of carbon surrounding the polyene and cumulene sp chains, thus forming graphitic nanodomains whose presence modify the Raman spectrum and, in particular, strong increase intensity of the D and G bands.

The last group of peaks between around 2300 and 3500 cm⁻¹ is due to the second-order mode of graphite (graphitized materials) [25].

By the way the increase of maximum of bands ratio D_1/D_4 can be interpreted as decrease of ionic impurities content that is confirmed by elemental analysis (Table 2). It is clear that such decrease should cause the decrease the scattering of current carries on ionized impurities and changes if electron structure of activated carbon (particularly $N(E)$ too).

One of most interesting effects, which were revealed, is the disappearing of C peak after ultrasonic treatment that is supposed to be related with above mentioned of more ordering of carbon bonds that results in abrupt intensity reduction for band that corresponds to stretching modes of linear sp -hybridized carbon structures.

A deeper understanding of the stability of sp carbon structures and of their role in the nanostructured carbon network would

provide a new insight in the physics and chemistry to produce the new forms of carbon with tailored structural and functional properties.

The change of phonon spectrum and as results the change of current carries scattering mechanism due to ultrasonic irradiation beside the above mentioned factors is also confirmed by existence of second order of Raman spectrum (2200 - 3700 cm^{-1}), which is caused by collection overtones of 1350 and 1550 cm^{-1} modes and their combination. By fitting of Lorentz curves to this spectrum we have identified the five bands (Fig. 12) from which the transformation of 2G bond to 2D₂ bond follows. Unfortunately we can pronounce only this fact, whose nature is not clarified at present time.

4. Conclusions

1. Ultrasonic modification of carbon, proposed in this work is suitable, cheap and effective method to increase the specific capacitance as well as power of carbon-based supercapacitors.
2. Significant improvement of properties, determining the practical use is found to be caused by essential reduction of time constant $R_{SC}C_{SC}$ – chain of VCR after ultrasonic irradiation, in particular R_{SC} .
3. Changes of parameters of double electric layer are tightly related with change of fractal dimension which at such parameters of ultrasonic treatment increase the percolate mobility of charge carries.
4. This method allows also controlling successfully the admixture and native defects distribution, existing on material surface and which are responsible for the surface electron states formation.

References

- [1] L.A. Dobrzański, Report on the main areas of the materials science and surface engineering own research, Journal of Achievements in Materials and Manufacturing Engineering 49/2 (2011) 514-549.
- [2] L.A. Dobrzański, M. Pawlyta, A. Hudecki, Conceptual study on a new generation of the high-innovative advanced porous and composite nanostructural functional materials with nanofibers, Journal of Achievements in Materials and Manufacturing Engineering 49/2 (2011) 550-565.
- [3] Chi-Chang Hu, Wen-Yar Li, Jeng-Yan Lin, The capacitive characteristics of supercapacitors consisting of activated carbon fabric-polyaniline composites in NaNO_3 , Journal of Power Sources 137 (2004) 152-157.
- [4] Feng-Chin Wu, Ru-Ling Tseng, Chi-Chang Hu, Chen-Ching Wang, Effects of pore structure and electrolyte on the capacitive characteristics of steam- and KOH-activated carbons for supercapacitors, Journal of Power Sources 144 (2005) 302-309.
- [5] K. Kierzek, E. Frackowiak, G. Lota, G. Gryglewicz, J. Machnikowski, Electrochemical capacitors based on highly porous carbons prepared by KOH activation, Electrochimica Acta 49 (2004) 515-523.
- [6] A.B. Fuertes, F. Pico, J.M. Rojo, Influence of pore structure on electric double-layer capacitance of template mesoporous carbons, Journal of Power Sources 133 (2004) 329-336.
- [7] M.W. Verbrugge, P. Liu, S. Soukiazian, Activated-carbon electric-double-layer capacitors: electrochemical characterization and adaptive algorithm implementation, Journal of Power Sources 141 (2005) 369-385.
- [8] K. Rajendra Prasad, N. Munichandraiah, Electrochemical studies of polyaniline in a gel polymer electrolyte, High energy and high power characteristics of a solid-state redox supercapacitor, Electrochemical and Solid-State Letters 5 (2002) A271-A274.
- [9] A. Malinauskas, J. Malinauskiene, A. Ramanavicius, Conducting polymer-based nanostructured materials: electrochemical aspects, Nanotechnology 16 (2005) R51-R62.
- [10] A. Nishino, A. Yoshida, I. Tanahashi, I. Tajima, M. Yamashita, T. Muranada, H. Yoneda, Planar capacitors with electrical double layer with polarizable electrodes made of activated carbon fiber, National Technical Report 31 (1985) 318-330.
- [11] B.E. Conway, Electrochemical supercapacitors. Plenum Publishing, New York, 1999.
- [12] Songhun Yoon, Jinwoo Lee, Taeghwan Hyeon, Seung M. Oh, Electric double-layer capacitor performance of a new mesoporous carbon, Journal of The Electrochemical Society 147 (2000) 2507-2512.
- [13] H. Gerischer, An interpretation of the double layer capacity of graphite electrodes in relation to the density of states at the Fermi level, The Journal of Physical Chemistry 89 (1985) 4249-4251.
- [14] B.A. Agranat, M.N. Dubrovin, N.N. Khavskii, G.I. Eskin, Fundamentals of physics and technologies of ultrasound, Vysshaya Shkola, Moskva, 1987.
- [15] I.V. Ostrovskii, A.B. Nadochii, A.A. Podolyan, Ultrasound stimulated low-temperature redistribution of impurities in silicon, Fizika i tekhnika poluprovodnikov 36 (2002) 389-391.
- [16] I.V. Zolotukhin, Yu.E. Kalinin, V.I. Loginova, Solid-state fractal structures, International Scientific Journal for Alternative Energy and Ecology 9 (2005) 56-66.
- [17] G. Porod, X-ray low angle scattering of dense colloid systems, Part I, Kolloid-Zeitschrift 124 (1951) 83-114.
- [18] R. de Levie, On porous electrodes in electrolyte solutions, Electrochimica Acta 8 (1963) 751-780.
- [19] Jaeyun Kim, Jinwoo Lee, Taeghwan Hyeon, Direct synthesis of uniform mesoporous carbons from the carbonization of as-synthesized silica/triblock copolymer nanocomposites, Carbon 42 (2004) 2711-2719.
- [20] A.B. Fuertes, S. Alvarez, Graphitic mesoporous carbons synthesised through mesostructured silica templates, Carbon 42 (2004) 3049-3055.
- [21] J. Robertson, Hard amorphous (diamond-like) carbons, Progress in Solid State Chemistry 21 (1991) 199-333.

- [22] M. Armandi, B. Bonelli, I. Bottero, C. Otero Areán, E. Garrone, Synthesis and characterization of ordered porous carbons with potential applications as hydrogen storage media, *Microporous and Mesoporous Materials* 103 (2007) 150-157.
- [23] L. Ravagnan, F. Siviero, C. Lenardi, P. Piseri, E. Barborini, P. Milani, Cluster-beam deposition and in situ characterization of carbyne-rich carbon films, *Physical Review Letters* 89 (2002) 285506.
- [24] A.C. Ferrari, J. Robertson, Interpretation of Raman spectra of disordered and amorphous carbon, *Physical Review B* 61 (2000) 14095-14107.
- [25] A.C. Ferrari, J. Robertson, Resonant Raman spectroscopy of disordered, amorphous, and diamondlike carbon, *Physical Review B* 64 (2001) 075414.